Recent progress in understanding Mars' unusual annular polar vortices

Stephen Hughes, William J. M. Seviour, Jemma Shipton and Stephen I. Thomson
Department of Mathematics and Statistics, University of Exeter, UK

Introduction

On Mars, Earth and several other bodies in the solar system, rapidly rotating flows exist in the winter polar regions. These are generally referred to as polar vortices, and though there can be confusion about their definition (Waugh, 2023), it is useful to study them and understand their impacts on polar atmospheric dynamics and chemistry.

In this review, we use the definition of a polar vortex given by Mitchell (2021), which is that they are coherent regions with absolute potential vorticity (PV) that is larger than the planetary PV and are centred on or near the pole. Alternative definitions based on, for example, wind or temperature can be used, but PV is the most common, and often the most useful, quantity to consider (Hoskins *et al.*, 1985). PV is defined as

$$q = \frac{\zeta_a \cdot \nabla\theta}{\rho}, \qquad (1)$$

where ζ_a is the absolute vorticity, $\nabla\theta$ is the vertical potential temperature gradient and ρ is the fluid density (Vallis, 2017), and it is materially conserved for adiabatic, frictionless flows.[1] This means that, without external forcing, a fluid parcel's PV will remain constant while it is transported through the atmosphere, allowing for tracing of the evolution of the polar vortex. Large gradients of PV are known to provide a barrier to mixing (Haynes and Shuckburgh, 2000), meaning that if a polar vortex is defined in terms of PV, the local mixing properties can often be inferred. The edge of a polar vortex is commonly seen to have such a large PV gradient and the resulting mixing barrier can have important consequences for polar chemistry, with one particularly notable example being the trapping of cold air within Earth's Southern Hemisphere polar vortex, which contributed to a significant depletion of ozone in this region: the ozone hole (e.g. Schoeberl and Hartmann, 1991).

The existence of a region of polar cyclonic flow can be reasoned through simple conservation of angular momentum. However, it should be noted that this is not always the mechanism that produces and maintains the polar vortex. At a very fundamental level, air at the equator is further from the axis of rotation than air at the pole, so its angular momentum is higher. When this air moves poleward due to, for example, the Hadley circulation, it is deflected in an eastward direction to conserve angular momentum, thus generating cyclonic flow in the polar regions. On Mars, as on Earth, atmospheric circulation is driven by the need to balance solar heating and radiative fluxes, generating meridional transport of air from low to high latitudes (Read *et al.*, 2015). This leads to a Hadley cell, as illustrated in Figure 1; on the poleward edge of this, we find a region of air that is defined as Mars' polar vortex.

Apart from Earth, Mars has the most studied planetary atmosphere and polar vortices, so provides an excellent opportunity to study familiar atmospheric features in a different scenario. With a similar obliquity (axial tilt) to Earth and an orbital eccentricity that is slightly higher, Mars' seasonal cycle is not dissimilar to that which we are accustomed to; the length of a Martian day (known as a 'sol') is only a little over 24h; and Mars' Rossby number is comparable to Earth's, giving a similar balance between rotation and advection in governing circulation patterns. There are also important differences between the two planets: a Martian year is almost twice the length of Earth's (the time of year is denoted though Solar Longitude (L_s), with $L_s = 0°$ corresponding to Northern Hemisphere spring equinox, $L_s = 90°$ giving northern summer solstice, and so forth); Mars' surface temperature averages only 210K, with average surface pressure of just 6.1hPa; and the major atmospheric constituent, making up 95.1% of Mars' atmosphere, is carbon dioxide (CO_2). Due to having a higher eccentricity than Earth, Mars does experience a stronger asymmetry in the seasonal cycle, and with perihelion (point of closest approach to the sun) occurring shortly before northern winter solstice, the increased solar irradiation leads to stronger atmospheric circulation during northern winter (Newman *et al.*, 2005). This is exacerbated by a large variation in topography between the two hemispheres, with the zonal mean elevation in the Southern Hemisphere ~3km higher than the Northern Hemisphere, leading to stronger convective activity, and hence stronger atmospheric circulation, during northern winter (Takahashi, 2003).

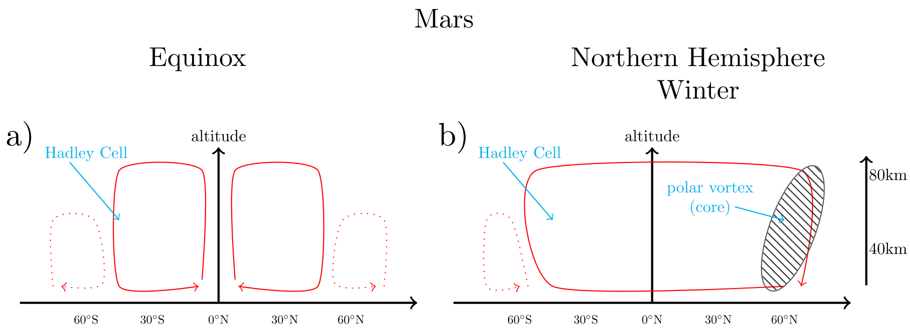

Figure 1. Schematic of the large-scale atmospheric circulation on Mars, showing the climatology of the Hadley cell and polar vortex. (a) Meridional circulation near the time of the equinox, showing symmetry across the two hemispheres. (b) Meridional circulation during Northern Hemisphere winter, with a large cross-equator Hadley Cell shown. (Courtesy: Emily Ball.)

[1] Due to the $1/\rho$ factor in Equation (1), the magnitude of PV can increase rapidly with altitude, so a commonly used scaling is that which was introduced by Lait (1994) and reformulates the PV as

$$q_s = q\left(\frac{\theta}{\theta_0}\right)^{-(1+c_p/R)}, \qquad (2)$$

where θ_0 is an arbitrary reference potential temperature, and c_p/R is the ratio of specific heat at constant pressure to specific gas constant for the relevant atmosphere.

Weather – 9999, Vol. 99, No. 9

RMetS Royal Meteorological Society

Figure 2. *Top-down view of a section of Mars' North PLDs, where erosion has revealed layers below the most recent. This allows observations of the dust signature of the past Martian atmosphere. Image taken by NASA's Mars Reconnaissance Orbiter. (Credit: NASA/JPL-Caltech/UArizona.)*

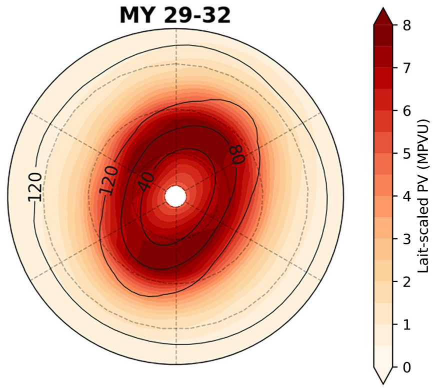

Figure 3. *Polar stereographic view of Northern Hemisphere winter (L_s = 255°–285°) average of Lait scaled PV (shading) and zonal winds (contours) on the 350K isentropic surface, averaged over MY 29–32 from the OpenMARS reanalysis dataset. The annular PV structure is clear, with a local minimum over the pole. Bounding latitude is 50°N. $1 MPVU = 100 PVU$, $1 PVU = 10^{-6} m^2 s^{-1} K kg^{-1}$. (Source: Mitchell (2021).)*

At Mars' poles, we find its polar layered deposits (PLDs) – the only known record of paleoclimate beyond our own planet, with an estimated age on the order of 10 million years (Smith, 2020). The PLDs, shown in Figure 2 for a section of the northern polar region, consist of layers of water ice interspersed with varying amounts of dust (Murray, 1972). The dust varies both in terms of absolute quantity and grain size, indicating differences in polar atmospheric dynamics over time. Given the importance of the polar vortex in governing transport into polar regions, by understanding its behaviour we may gain insights into the causes of differences between layers in the PLDs, recently listed as one of the top priorities for Martian research by a Mars exploration advisory group (Banfield, 2020).

Recognition of the broader importance of Mars' polar vortices has motivated several recent advances. Here we review these advances and outstanding questions, regarding the structure of Mars' polar vortices and how this affects atmospheric transport. In the "Observations, reanalysis and comprehensive modelling" Section, we will give an overview of observations and comprehensive modelling studies of Martian polar vortices. We will then, in the "Idealised modelling" Section, describe some idealised modelling work aiming to answer some of the issues raised by more realistic simulations. Finally, we will conclude with suggestions of directions for further study in the "Conclusions and outlook" Section.

Observations, reanalysis and comprehensive modelling

There have been *in situ* observations of Mars for many years, since the first successful spacecraft mission in 1964. With this wealth of observational data available, it has been possible to create reanalysis datasets for the Martian atmosphere. Reanalysis datasets combine climate models with observations, using the models to fill the spatial and temporal gaps between observations, and using the observations to constrain the models as closely as possible to the real atmospheric state. Currently, three main global Martian reanalysis products exist – MACDA (Montabone, 2014), EMARS (Greybush, 2019) and OpenMARS (Holmes *et al*., 2020).[2] MACDA, EMARS and OpenMARS all assimilate temperature and dust column opacity values, with OpenMARS also including water vapour column and vertical profiles and ozone column values. In order to produce these reanalysis datasets, Martian Global Climate Models (MGCMs) are needed, and there are an increasing number of these available. MACDA and OpenMARS use the spectral version of the Mars Planetary Climate Model (Mars PCM) developed at LMD (Paris), the University of Oxford and The Open University (Forget, 1999). EMARS uses the NASA-GFDL MGCM (Haberle, 2019).

Using reanalysis datasets, there have been multiple studies of the climatology of the Martian polar vortices (Mitchell, 2015, 2021; Waugh, 2016, 2023). A consistent finding between all of these studies is that the Martian polar vortices have an annular PV structure. This means that they have a local minimum of PV over the pole, with a ring of higher PV around this, as shown in Figure 3. Following theoretical

[2] A fourth, the LMD-LETKF reanalysis dataset (Young, 2022), also exists but only covers specific short time periods so is less useful here. An updated version of MACDA is in preparation (Ruan, 2021; Read, 2022); however, data are not yet publicly available.

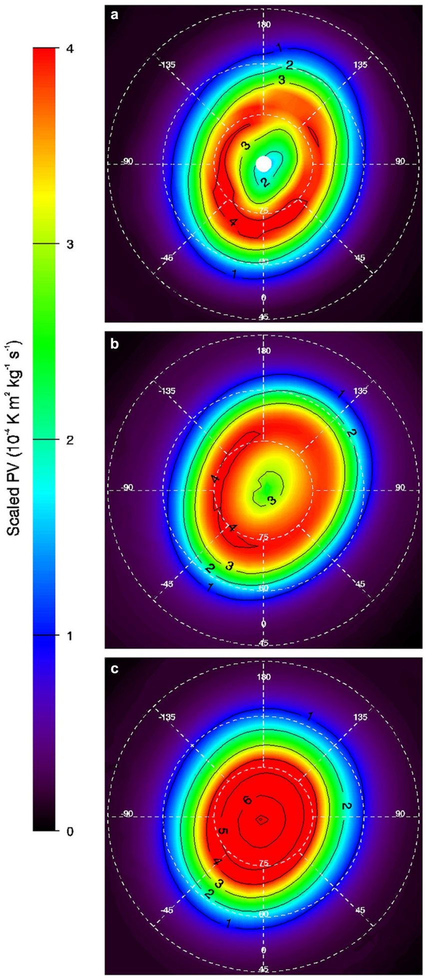

Figure 4. *North polar stereographic projection of Lait scaled PV on the 300K isentropic surface from (a) the MACDA reanalysis product, (b) a standard MarsWRF simulation, (c) MarsWRF with CO_2 microphysics removed. The different structures shown in (b) and (c) show the importance of CO_2 microphysics in producing the annular PV structure. Bounding latitude is 45°N. (Source: Toigo* et al. *(2017).)*

work by Rayleigh (1879) and Dritschel and Polvani (1992), it is known that a strip of PV, on a plane and sphere, respectively, is barotropically unstable. The gradients in PV on either side of the strip support counter-propagating Rossby waves, which grow in amplitude until the strip breaks up. On a sphere, the stable state is for PV to increase monotonically towards the pole (a 'monopolar' structure); this is the expected PV structure of a polar vortex and is what is generally observed in Earth's stratosphere. It is therefore clear that there must be a forcing term present to produce and maintain the annulus in Mars' polar vortices. As mentioned in the "Introduction" Section, Mars' atmosphere is predominantly CO_2; significantly, the atmospheric temperature often falls below the condensation (strictly speaking, sublimation) point of CO_2 during winter in polar regions. This leads to condensation of CO_2 within the atmosphere, releasing large amounts of latent heat, a diabatic heating source. Referring to Equation (1), atmospheric heating decreases the vertical gradient in potential temperature, and so locally decreases the PV. Modelling work by Toigo *et al.* (2017) demonstrated that when the effects of CO_2 condensation are removed from a MGCM (in this case the MarsWRF model), by disabling phase changes to avoid latent heat release, the polar vortex loses its annular structure. This is illustrated in Figure 4 with a clear difference evident between the reanalysis and full MGCM, and the MGCM with CO_2 microphysics removed.

In Figures 3 and 4, it can also be seen that the polar vortex displays an elliptical PV structure, with the PV annulus extending further equatorward around 150°E and 30°W. This orientation is consistent with forcing from stationary wavenumber-2 waves driven by topography, as described by, among others, Mitchell (2015), Waugh (2016), Streeter (2021), Mester (2022) and Alsaeed *et al.* (2024). This elliptical structure is a particularly notable feature in the Northern Hemisphere, with the Southern winter polar vortex (not shown here) displaying a more zonally uniform structure. Another key difference between the two hemispheres is that the northern polar vortex is typically stronger, with larger absolute values of PV (Waugh, 2016). This is due to the stronger meridional circulation that occurs during northern winter, as described in the "Introduction" Section, which leads to a faster westerly jet and higher values of PV. For this reason, all plots shown here are of the Northern Hemisphere winter polar vortex.

While it is generally accepted that the time-average Martian polar vortex is annular and elliptical, as shown in Figure 5(a), with significant forcing coming from CO_2 condensation, more questions arise when looking at snapshots of Martian polar PV. The random snapshot of reanalysis data in Figure 5(b) shows much larger spatial variability with the vortex 'ring' now made up of several 'blobs' of higher and lower PV. These blobs rotate cyclonically around the pole to give an annulus in the time average. It is useful to compare snapshots of PV between different reanalysis products and MGCMs in order to improve understanding of the instantaneous PV structure. Figure 6 shows PV snapshots from two reanalysis datasets and one MGCM. The most obvious difference here is that both reanalysis datasets show spatial patchiness in the PV (although in different amounts), while the MGCM PV is much smoother. This result is consistent across a variety of reanalyses and

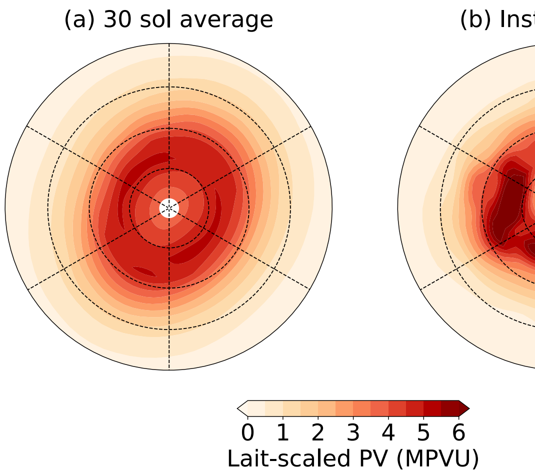

Figure 5. North polar stereographic projection of Lait scaled PV on the 300K isentropic level for (a) a 30sol average near $L_s = 270°$, and (b) instantaneously at $L_s = 270°$ in MY 29 from the OpenMARS reanalysis dataset. The patchiness of the instantaneous PV field compared to the time average is clearly seen. The plots are bounded at a latitude of 50°N.

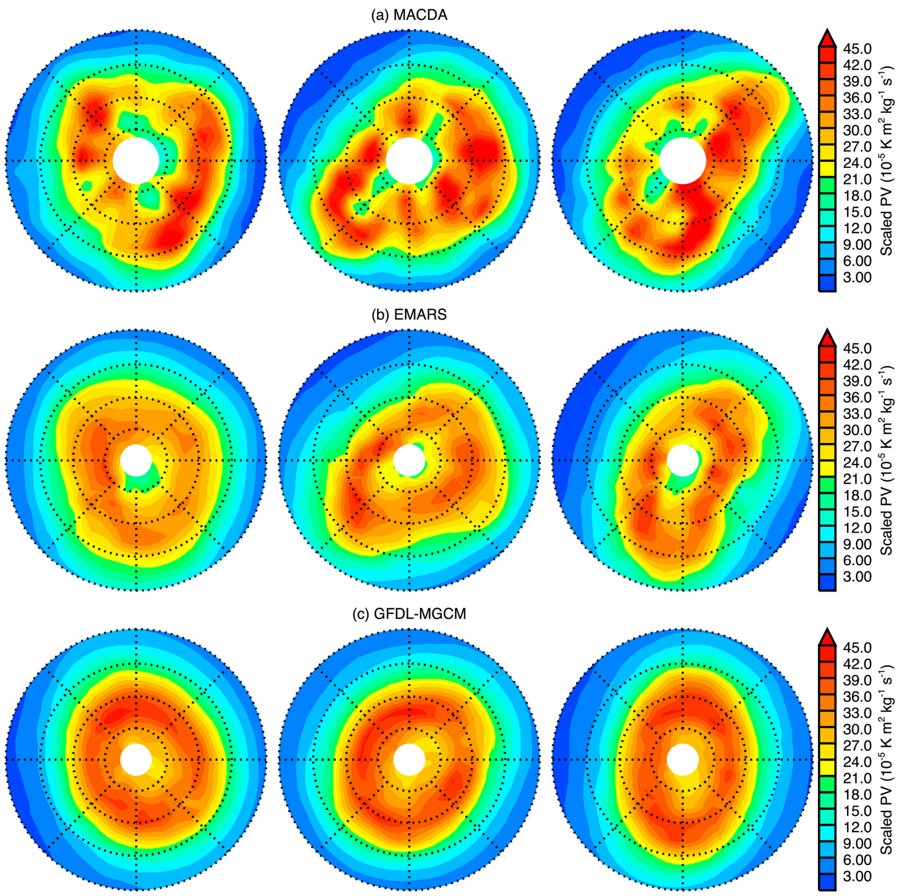

Figure 6. North polar stereographic maps of instantaneous Lait scaled PV on the 300K isentropic level from (a) MACDA reanalysis, (b) EMARS reanalysis, (c) GFDL MGCM; the difference in patchiness between reanalysis and the MGCM is evident. Each row shows plots 1sol apart near $L_s = 216°$, they are bounded at 50°N. (Source: Waugh (2016).)

MGCMs, and raises the question of whether the PV patchiness is a physical feature or whether it is being spuriously generated in the reanalysis process. Similar PV blobs were found in early analysis datasets of Earth (e.g. McIntyre and Palmer, 1983), whereas the modern equivalents do not show these features (Waugh, 2023); McIntyre and Palmer (1983) compared older datasets to looking through a 'pane of knobbly glass' due to their coarse resolution and sparsity of observations, which led to the appearance of blobs of PV. Thus, it is possible that, in time, the quality of the Martian reanalyses will improve, with more observational data and higher model resolution, and the PV patchiness may disappear. The analysis datasets used by McIntyre and Palmer (1983) had a resolution of roughly 8°, which is of the same order of magnitude as current Mars reanalyses (5°), and much coarser than modern Earth reanalyses (0.25°).

It is not entirely unexpected, however, that Mars' polar vortices should contain blobs of PV, given the presence of processes that do not occur on Earth. Firstly, the barotropic instability that the PV annulus is subject to could contribute to forming the patches. Further, Mars also has two processes that occur on a small spatial scale and may impact the polar vortex structure: variability in the previously mentioned CO_2 condensation, which will be discussed in the "Idealised modelling" Section, as well as local dust storms. One of Mars' most distinctive features is the prevalence of dust on its surface and in its atmosphere. As described by Newman (2022), dust on Mars has a comparable effect on atmospheric circulation to the water cycle in Earth's atmosphere, with strong radiative forcing making the dust a significant factor. While there is a constant background amount of airborne dust with its own seasonal cycle, the most notable effects on the polar vortices come from dust storms. These can be either local, regional or global, in order of increasing spatial and temporal extent. Work by Guzewich *et al*. (2016), Ball (2021) and Streeter (2024) has shown that, in observations and MGCMs, the average effect of increased atmospheric dust loading is to decrease polar vortex strength and move the latitude of maximum PV polewards; that is, 'shrink' the polar vortex. This occurs due to the Hadley Cell's poleward edge moving further poleward and therefore reducing the latitudinal extent of the PV annulus; in cases of extremely high dust loading, for example during a global dust storm (GDS), the polar vortex loses its annular structure entirely and instead PV increases monotonically to the pole. Guzewich *et al*. (2016) show that despite the Hadley Cell strengthening during a GDS, zonal wind speeds and thus PV decrease, thought to be due to altered eddy activity. While most of these studies have focussed on the zonal mean response, Streeter (2021) and Alsaeed *et al*. (2024) found a longitudinally varying response to a GDS, with the poleward shift of the northern polar vortex moving it away from regions of topography-induced wavenumber-2 forcing, thus reducing its ellipticity. Future studies of reanalysis and MGCMs to investigate responses in local overturning and PV structures due to global, and smaller scale, dust storms may provide further insights into polar vortex variability and consequences on atmospheric mixing.

As well as quantifying the effects of dust on the polar vortex, the motivation of deciphering the PLDs means that it is of interest to know how the polar vortex controls the transport of dust into polar regions. Ball *et al*. (2023) investigated the changing horizontal mixing properties of the vortex under changing obliquity, eccentricity and dust loading in a MGCM. They found that, in general, an annular vortex has a mixing barrier on its equatorward edge, where PV gradients are largest, while mixing is larger in the midlatitudes in what is referred to as the 'surf zone' following McIntyre and Palmer (1983).

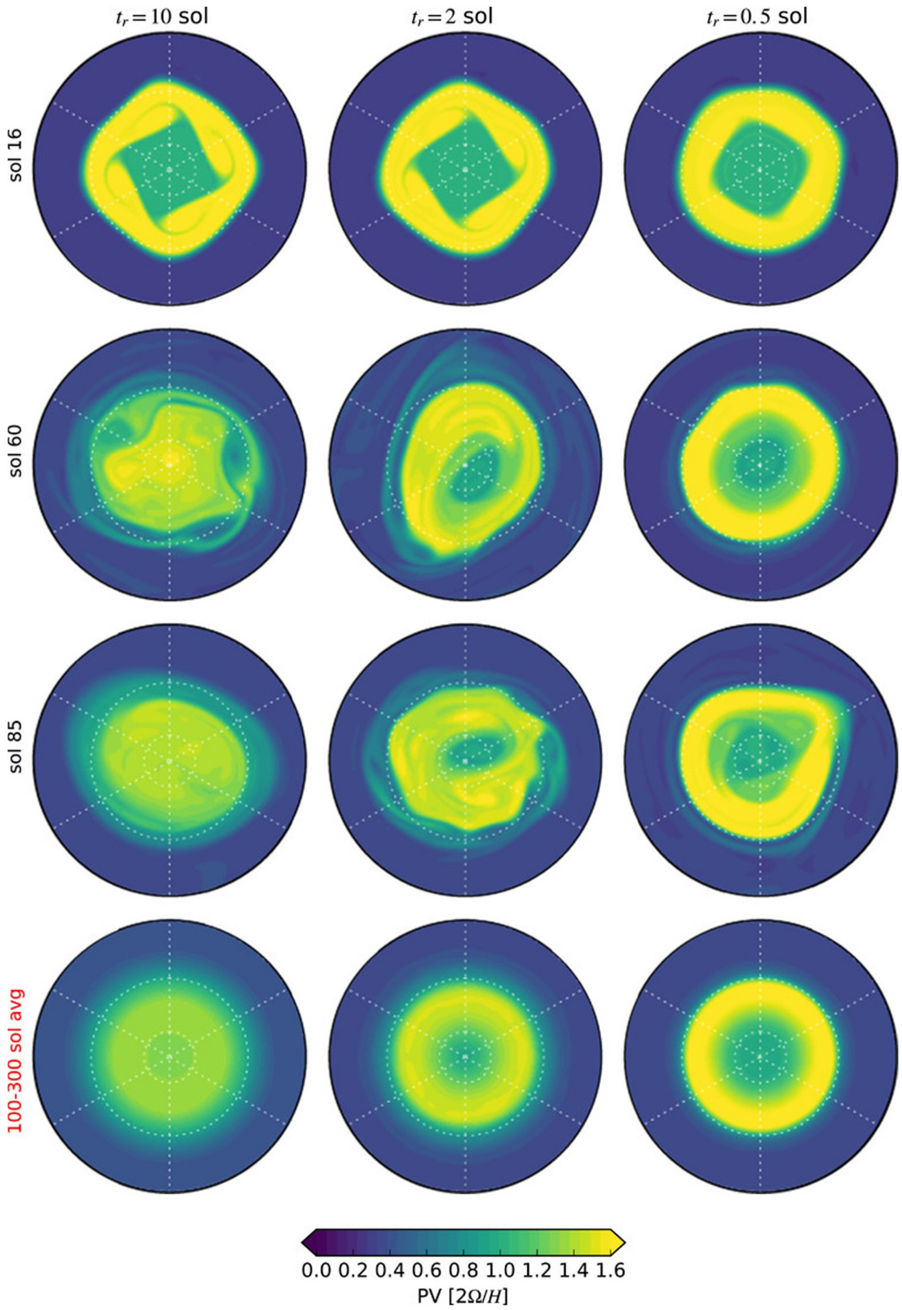

Figure 7. Polar stereographic projection of (top three rows) PV evolution and (bottom) 100–300sol PV time average in a shallow water model with relaxation towards an annular PV profile. The timescale t_r for the relaxation term is (left) 10sol, (middle) 2sol, (right) 0.5sol. The initial breakup of the annulus is visible with all three timescales; only the shorter relaxation times produce an annulus in the long-term time average demonstrating the necessary. Plots are bounded at 40°N. (Source: Seviour et al. *(2017).)*

This is a similar pattern to that found in studies of Earth's stratospheric polar vortices. Changes in obliquity and dust loading, as may have happened in Mars' past, are found to have significant effects, with the mixing barrier in the Northern Hemisphere even disappearing in some cases. Similar findings were made by Shultis (2025) when changing the PV profile of the polar vortex in another MGCM. They showed that both monopolar and annular polar vortices have mixing barriers on the equatorward edge of the polar vortex, where the PV gradient is largest. They found more of a difference in the horizontal mixing properties in the interior of the polar vortex, where annular PV structures allowed for stronger mixing within the annulus, while monopolar vortices displayed little mixing within the region of higher PV.

Clearly, the exact morphology of the polar vortex can have a large impact on its mixing properties and how it governs the transport of airborne dust and trace gases into polar regions. Studies of water transport across the northern polar vortex by Gillespie (2024) using an MGCM and reanalysis data also support this. In the MGCM, where the polar vortex is a smooth annulus, a strong mixing barrier is found with little water vapour crossing the polar vortex edge. Meanwhile, in the reanalysis data, where the polar vortex is more instantaneously spatially patchy, greater levels of cross-vortex transport are found. Although no work was done to directly attribute the increased transport to a more patchy vortex, it is reasonable to suppose that, because a patchy vortex contains regions with smaller meridional PV gradients, it will contain regions of increased cross-vortex transport. Thus, the extent to which the polar vortex is patchy may be a key factor in explaining the varying dust amounts in the PLDs, potentially providing insights into past Martian climate.

Idealised modelling

In order to improve understanding of the polar vortex structure and patchiness, a hierarchy of modelling approaches have been used. While comprehensive models aim to provide an accurate description of a planetary atmosphere, it can be easier to directly attribute responses to their causes by stripping a system back to its fundamental processes and removing complicated feedbacks. This is where idealised models come in. One of the most common types of idealised models used for studying planetary atmospheres is a 'shallow water' setup, based on the shallow water equations (see e.g. Vallis, 2017) which model a single layer of incompressible fluid with no vertical structure but full horizontal dynamics. Shallow water models have been widely used to model Earth's stratospheric polar vortex (e.g. Juckes, 1989; Norton, 1994; Rong and Waugh, 2004; Liu and Scott, 2015; Scott, 2016), and have more recently been applied to the Martian polar vortices as well (Seviour *et al*., 2017; Rostami *et al*., 2018; Scott *et al*., 2020).

The focus of Seviour *et al*. (2017) was to determine if an annular vortex could be made to persist by including basic forcing terms. Having shown that, in a free running shallow water model, an initially annular vortex would break up and form a monopolar structure (verifying the barotropic instability work by Dritschel and Polvani, 1992), they included a relaxation term towards an annular structure. By varying the timescale of this relaxation (essentially controlling the relaxation strength) they found that the minimum timescale required to maintain an annular vortex was around 0.5–2sols, as illustrated in Figure 7. This agrees with theoretical work by Eckermann *et al*. (2011), who found the radiative relaxation timescale of the Martian atmosphere to be 0.5–2sols.

The work by Rostami *et al*. (2018) developed these ideas further, by including a representation of spatially variable CO_2 condensation with the aim of investigating if this could locally destroy PV and lead to increased PV patchiness. The key difference was the inclusion of a forcing term, activated by the presence of high dust concentration (acting as condensation nuclei) and low pressure, which locally increases the strength of relaxation towards an annulus; this is analogous to the effect of latent heating from CO_2 condensation. They found, similarly to Seviour *et al*. (2017), that including only a uniform relaxation towards an annulus would produce a smooth stable annular polar vortex. By adding the CO_2 condensation term, they were able to increase the patchiness of this vortex, meaning the results more closely match the findings of reanalysis data; this is shown in Figure 8. Further adaptations to this model could more closely match the conditions on Mars: here the 'background relaxation' term is towards an annular vortex, while on Mars it is thought that without the CO_2 condensation, the vortex would have a stable monopolar PV profile. Additionally, work by Alsaeed and Hayne (2022) suggests that water ice molecules may act as condensation nuclei. Given that their number density far outweighs that of CO_2, the availability of condensation nuclei should not be a limiting factor in CO_2 condensation, as it is within the model of Rostami *et al*. (2018). Further idealised modelling experiments which separate the background relaxation towards a stable monopolar profile from the postulated CO_2-related local destruction of polar PV may prove useful.

Having seen that it is possible to represent the Martian annular polar vortex

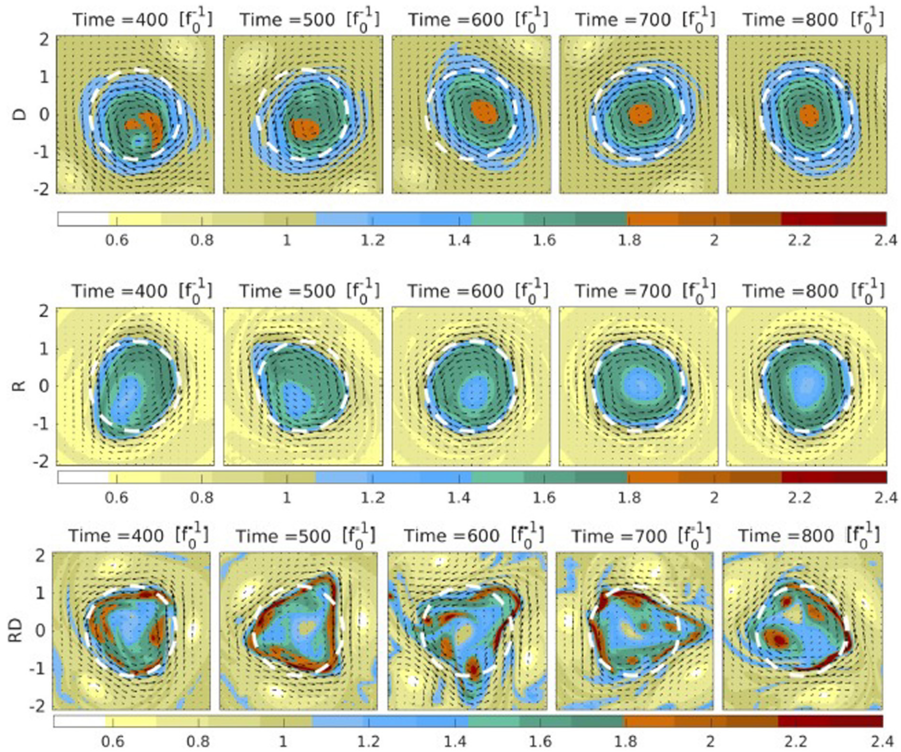

Figure 8. Plots of PV evolution in a shallow water model with relaxation terms representing (D) CO_2 'condensation' only, (R) 'radiative' relaxation towards an annular PV profile, (RD) both terms in conjunction. We see the radiative relaxation is necessary to maintain an annular profile, while the addition of CO_2 condensation produces blobs of PV. PV and time are shown in scaled units relevant to the model. The white dashed lines shows initial radius of maximum zonal wind, that is, the edge of the initial PV annulus. (Source: Rostami et al. *(2018).)*

in a shallow water model, it is of interest to study the transport properties of these configurations. Work by Shultis (2025) found that the shallow water setup of Seviour *et al*. (2017) exhibits similar transport properties to MGCMs, with a mixing barrier on the equatorward edge of the PV annulus and increased mixing inside the polar vortex and in the surf zone. By varying the relaxation profile, they were able to test transport with different PV structures. The findings were as expected; for example, a thicker annulus provides a larger mixing barrier, a weaker relaxation term produces a less smooth vortex with increased mixing across it, and removing the relaxation term entirely gives a monopolar structure with significant mixing occurring only in the surf zone outside the polar vortex.

Interestingly, similar findings were made by Hendricks and Schubert (2009) focussing on a very different context. They studied unstable annuli of vorticity (rather than PV) in a 2D model, replicating structures seen in the eyewall of strong and intensifying hurricanes. They found that, much like a PV annulus, an annulus of vorticity provides a mixing barrier while there are increased mixing rates inside and outside the annulus. With important consequences for the growth phase of hurricanes, this is another example of the importance of understanding the transport properties of barotropically unstable annuli of PV and vorticity. The similarity between the results described above highlights the generality of geophysical fluid dynamics, with phenomena of vastly differing scales exhibiting the same behaviour, and allowing understanding of one feature to be applied to a broader context.

Conclusions and outlook

Mars, like Earth, is observed to have a polar vortex in its winter hemisphere, with a strong westerly flow and elevated levels of PV. Surprisingly, the Martian polar vortices exist in a barotropically unstable state: an annulus of PV with a local minimum over the pole and a ring of higher PV around this. Work over the last decade using reanalysis data, MGCMs, and idealised models, has developed a good physical understanding of this phenomenon. Latent heat release due to condensation of atmospheric CO_2 is thought to be the primary driver of this annular structure, with the modification of vertical potential temperature gradients leading to destruction of PV over the pole. This is supported by comprehensive modelling studies, where the removal of CO_2 microphysics leads to a monopolar polar vortex with PV increasing monotonically towards the pole. Idealised models have also been able to maintain an annular structure through simple relaxation terms with timescales similar to those characteristic of the Martian atmosphere. Reanalysis data shows the polar vortex as instantaneously spatially patchy, disagreeing with MGCMs, which show a much smoother annulus; idealised models suggest that spatially variable CO_2 condensation could be responsible for this patchiness. Further work is required to improve understanding of the patchiness, firstly to determine if it is a real physical feature or simply an artefact of the reanalysis. If it is shown to be a real feature then further modelling studies may help determine the cause(s) of the patchiness.

Large PV gradients, such as those associated with the polar vortex edge, are known to have significant impacts on atmospheric transport; previous work shows that annular and monopolar PV structures both have a mixing barrier on the equatorward edge of the polar vortex, at the location of maximum PV gradient, with a surf zone of increased mixing at lower latitudes than this. The interior of an annular polar vortex is shown to have more horizontal mixing than a monopolar structure. A patchy polar vortex may display notably different atmospheric mixing to a smooth one, due to the changing presence of large PV gradients. Thus, further studies of the transport properties of different annuli of PV may help provide insights into the formation of, and variation within, the Martian PLDs. If links are made between dust deposits and polar vortex morphology, this may prove a significant advance in using the PLDs as a signature of different atmospheric states in Mars' past, one of the major challenges of Martian science (Smith, 2020).

Author contributions

Stephen Hughes: Conceptualization; writing – original draft; writing – review and editing. **William J. M. Seviour:** Conceptualization; supervision; writing – review and editing. **Jemma Shipton:** Supervision; writing – review and editing. **Stephen I. Thomson:** Supervision; writing – review and editing.

Acknowledgements

The authors would like to thank two anonymous reviewers for their insightful feedback on drafts of this paper and would also like to thank Emily Ball for Figure 1. This work forms part of a PhD studentship funded by the Science and Technology Facilities Council. Permission has been obtained from Wiley for Figures 4 and 6, Elsevier for Figure 8 and AMetSoc for Figure 7.

Data availability statement

Data sharing is not applicable to this article as no new data were created or analysed in this study.

References

Alsaeed NR, **Hayne PO**. 2022. Transport of water into the polar regions of Mars through scavenging by CO_2 snowfall. *J. Geophys. Res. Planets* **127**(11): e2022JE007386. https://doi.org/10.1029/2022JE007386

Alsaeed NR, **Hayne PO**, **Concepcion V**. 2024. Seasonal and inter-annual variability in the polar vortex and snowfall on Mars. *J. Geophys. Res. Planets* **129**(12): e2024JE008397. https://doi.org/10.1029/2024JE008397

Ball ER, **Seviour WJM**, **Mitchell DM**. 2023. The importance of isentropic mixing in the formation of the Martian polar layered deposits. *Planet. Sci. J.* **4**(11): 213. https://doi.org/10.3847/PSJ/AD045D

Ball ER. 2021. The roles of latent heating and dust in the structure and variability of the northern Martian polar vortex. *Planet. Sci. J.* **2**(5): 203. https://doi.org/10.3847/PSJ/ac1ba2

Banfield D. 2020. Mars Science Goals, Objectives, Investigations, and Priorities: white paper posted March, 2020 by the Mars Exploration Program Analaysis Group (MEPAG) at https://mepag.jpl.nasa.gov/reports.cfm

Dritschel DG, **Polvani LM**. 1992. The roll-up of vorticity strips on the surface of a sphere. *J. Fluid Mech.* **234**: 47–69. https://doi.org/10.1017/S0022112092000697

Eckermann SD, **Ma J**, **Zhu X**. 2011. Scale-dependent infrared radiative damping rates on Mars and their role in the deposition of gravity-wave momentum flux. *Icarus* **211**(1): 429–442. https://doi.org/10.1016/J.ICARUS.2010.10.029

Forget F. 1999. Improved general circulation models of the Martian atmosphere from the surface to above 80 km. *J. Geophys. Res. Planets* **104**(E10): 24155–24175. https://doi.org/10.1029/1999JE001025

Gillespie HE. 2024. Water transport in the Mars northern winter polar atmosphere: observations and simulations. *J. Geophys. Res. Planets* **129**(5): e2023JE008273. https://doi.org/10.1029/2023JE008273

Greybush SJ. 2019. The ensemble Mars atmosphere reanalysis system (EMARS) version 1.0. *Geosci. Data J.* **6**(2): 137–150. https://doi.org/10.1002/GDJ3.77

Guzewich SD, **Toigo AD**, **Waugh DW**. 2016. The effect of dust on the Martian polar vortices. *Icarus* **278**: 100–118. https://doi.org/10.1016/j.icarus.2016.06.009

Haberle RM. 2019. Documentation of the NASA/Ames Legacy Mars Global Climate Model: simulations of the present seasonal water cycle. *Icarus* **333**: 130–164. https://doi.org/10.1016/j.icarus.2019.03.026

Haynes P, **Shuckburgh E**. 2000. Effective diffusivity as a diagnostic of atmospheric transport: 1. Stratosphere. *J. Geophys. Res. Atmos.* **105**(D18): 22777–22794. https://doi.org/10.1029/2000JD900093

Hendricks EA, **Schubert WH**. 2009. Transport and mixing in idealized barotropic hurricane-like vortices. *Q. J. R. Meteorol. Soc.* **135**(643): 1456–1470. https://doi.org/10.1002/qj.467

Holmes JA, **Lewis SR**, **Patel MR**. 2020. OpenMARS: a global record of Martian weather from 1999 to 2015. *Planet. Space Sci.* **188**: 104962. https://doi.org/10.1016/J.PSS.2020.104962

Hoskins BJ, **McIntyre ME**, **Robertson AW**. 1985. On the use and significance of isentropic potential vorticity maps. *Q. J. R. Meteorol. Soc.* **111**(470): 877–946. https://doi.org/10.1002/qj.49711147002

Juckes M. 1989. A shallow water model of the winter stratosphere. *J. Atmos. Sci.* **46**(19): 2934–2956. https://doi.org/10.1175/1520-0469(1989)046%3C2934:ASWMOT%3E2.0.CO;2

Lait LR. 1994. An alternative form for potential vorticity. *J. Atmos. Sci.* **51**(12): 1754–1759. https://doi.org/10.1175/1520-0469(1994)051<1754:AAFFPV>2.0.CO;2

Liu YS, **Scott RK**. 2015. The onset of the barotropic sudden warming in a global model. *Q. J. R. Meteorol. Soc.* **141**(693): 2944–2955. https://doi.org/10.1002/qj.2580

McIntyre ME, **Palmer TN**. 1983. Breaking planetary waves in the stratosphere. *Nature* **305**(5935): 593–600. https://doi.org/10.1038/305593a0

Mester M. 2022. Control of the oscillations of the Martian northern hemisphere polar vortex by the Hadley cell and topographic forcing. *Icarus* **382**: 115019. https://doi.org/10.1016/j.icarus.2022.115019

Mitchell DM. 2015. Polar vortices on earth and Mars: a comparative study of the climatology and variability from reanalyses. *Q. J. R. Meteorol. Soc.* **141**(687): 550–562. https://doi.org/10.1002/QJ.2376

Mitchell DM. 2021. Polar vortices in planetary atmospheres. *Rev. Geophys.* **59**(4): e2020RG000723. https://doi.org/10.1029/2020RG000723

Montabone L. 2014. The Mars analysis correction data assimilation (MACDA) dataset V1.0. *Geosci. Data J.* **1**(2): 129–139. https://doi.org/10.1002/gdj3.13

Murray BC. 1972. Geological framework of the south polar region of Mars. *Icarus* **17**(2): 328–345. https://doi.org/10.1016/0019-1035(72)90004-8

Newman CE, **Lewis SR**, **Read PL**. 2005. The atmospheric circulation and dust activity in different orbital epochs on Mars. *Icarus* **174**(1): 135–160. https://doi.org/10.1016/j.icarus.2004.10.023

Newman CE. 2022. 7.24 – Martian dust, in Treatise on Geomorphology, 2nd edn. Shroder J(J)F (ed). Academic Press, pp 637–666. https://doi.org/10.1016/B978-0-12-818234-5.00143-7.

Norton WA. 1994. Breaking Rossby waves in a model stratosphere diagnosed by a vortex-following coordinate system and a technique for advecting material contours. *J. Atmos. Sci.* **51**(4): 654–673. https://doi.org/10.1175/1520-0469(1994)051%3C0654:BRWIAM%3E2.0.CO;2

Rayleigh JWS. 1879. On the stability, or instability, of certain fluid motions. *Proc. Lond. Math. Soc.* **1**(1): 57–72. https://doi.org/10.1112/plms/s1-11.1.57

Read PL, **Lewis SR**, **Mulholland DP**. 2015. The physics of Martian weather and climate: a review. *Rep. Prog. Phys.* **78**(12): 125901. https://doi.org/10.1088/0034-4885/78/12/125901

Read PL. 2022. MACDA II: a new reanalysis for the Martian atmosphere using vertically-resolved dust opacity observations, in 7th Mars Atmosphere Modelling and Observations Workshop, Paris, France.

Rong P-P, **Waugh DW**. 2004. Vacillations in a shallow-water model of the stratosphere. *J. Atmos. Sci.* **61**: 1174–1185. https://doi.org/10.1175/1520-0469(2004)061%3C1174:VIASMO%3E2.0.CO;2

Rostami M, **Zeitlin V**, **Montabone L**. 2018. On the role of spatially inhomogeneous diabatic effects upon the evolution of Mars' annular polar vortex. *Icarus* **314**: 376–388. https://doi.org/10.1016/j.icarus.2018.05.026

Ruan T. 2021. Assimilation of both column- and layer-integrated dust opacity observations in the Martian atmosphere. *Earth Space Sci.* **8**(12): e2021EA001869. https://doi.org/10.1029/2021EA001869

Schoeberl MR, **Hartmann DL**. 1991. The dynamics of the stratospheric polar vortex and its relation to springtime ozone depletions. *Science* **251**(4989): 46–52. https://doi.org/10.1126/science.251.4989.46

Scott RK. 2016. A new class of vacillations of the stratospheric polar vortex. *Q. J. R. Meteorol. Soc.* **142**(698): 1948–1957. https://doi.org/10.1002/qj.2788

Scott RK, **Seviour WJM**, **Waugh DW**. 2020. Forcing of the Martian polar annulus by Hadley cell transport and latent heating. *Q. J. R. Meteorol. Soc.* **146**(730): 2174–2190. https://doi.org/10.1002/qj.3786

Seviour WJM, **Waugh DW**, **Scott RK**. 2017. The stability of Mars's annular polar vortex. *J. Atmos. Sci.* **74**(5): 1533–1547. https://doi.org/10.1175/JAS-D-16-0293.1

Shultis J. 2025. Transport and mixing in planetary polar vortices. *Planet. Sci. J.* **6**(3): 63. https://doi.org/10.3847/PSJ/adba4b

Smith IB. 2020. The holy grail: a road map for unlocking the climate record stored within mars' polar layered deposits. *Planet. Space Sci.* **184**: 104841. https://doi.org/10.1016/j.pss.2020.104841

Streeter PM. 2024. An eight-year climatology of the Martian northern polar vortex. *Icarus* **409**: 115864. https://doi.org/10.1016/j.icarus.2023.115864

Streeter PM. 2021. Asymmetric impacts on Mars' polar vortices from an equinoctial global dust storm. *J. Geophys. Res. Planets* **126**(5): e2020JE006774. https://doi.org/10.1029/2020JE006774

Takahashi YO. 2003. Topographically induced north-south asymmetry of the meridional circulation in the Martian atmosphere. *J. Geophys. Res. Planets* **108**: 5018. https://doi.org/10.1029/2001JE001638

Toigo AD, **Waugh DW**, **Guzewich SD**. 2017. What causes Mars' annular polar vortices? *Geophys. Res. Lett.* **44**(1): 71–78. https://doi.org/10.1002/2016GL071857

Vallis GK. 2017. Atmospheric and Oceanic Fluid Dynamics: Fundamentals and Large-Scale Circulation, 2nd edn. Cambridge University Press: Cambridge. https://doi.org/10.1017/9781107588417.

Waugh DW. 2016. Martian polar vortices: comparison of reanalyses. *J. Geophys. Res. Planets* **121**(9): 1770–1785. https://doi.org/10.1002/2016JE005093

Waugh DW. 2023. Fluid dynamics of polar vortices on Earth, Mars, and Titan. *Annu. Rev. Fluid Mech.* **55**(1): 265–289. https://doi.org/10.1146/annurev-fluid-120720-032208

Young RMB. 2022. First assimilation of atmospheric temperatures from the emirates Mars infrared spectrometer. *Geophys. Res. Lett.* **49**(21): e2022GL099656. https://doi.org/10.1029/2022GL099656

Correspondence to: S. Hughes
sh1293@exeter.ac.uk

doi: 10.1002/wea.7713